Enhancing ISAC Network Throughput Using Beyond Diagonal RIS

Zengrui Liu, Yang Liu, Shanpu Shen, Qingqing Wu, and Qingjiang Shi

***Abstract*—Emerging literature has shown that deploying reconfigurable intelligent surface (RIS) can remarkably promote integrated sensing and communication (ISAC) system's performance. Meanwhile, the emerging novel beyond-diagonal (BD)-RIS architecture has manifested its superior beamforming capability over the conventional diagonal RIS. This paper investigates utilizing fully-connected BD-RIS to improve ISAC system's throughput while ensuring sensing quality, By utilizing majorization-minimization (MM) and penalty-dual-decomposition (PDD) method, we develop an efficient algorithm to tackle the orthogonality condition and non-convex quartic inequality involving BD-RIS. Numerical results demonstrate the effectiveness of our solution and the benefit of BD-RIS deployment in ISAC network.**

***Index Terms*—Integrated sensing and communication (ISAC), reconfigurable intelligent surface (RIS), beyond diagonal RIS**

I. Introduction

Integrated sensing and communication (ISAC) is a key technology for the next-generation wireless communication system [1]-[2]. Inspired by the recent success of reconfigurable intelligent surface (RIS) in various applications, e.g., [3], a multitude of works investigate deploying RIS to improve ISAC system performance. As analyzed in [4], the deployment of RIS in radar systems can benefit target detection performance. Especially, when the line-of-sight (LoS) propagation path between the base station (BS) and the target is blocked, the sensing signal-to-noise-ratio (SNR) can be significantly elevated. It has been shown in [5] that leveraging RIS in a dual-functional radar-communication (DFRC) system can remarkably improve detection probability. The authors of [6] developed efficient algorithm to jointly optimize RIS configuration and power allocation in uplink ISAC system and manifested the benefit of deploying RIS. The latest work [7] has shown that appropriate configuration of RIS can significantly improve the performance of target's angle-of-arrival (AoA) estimation.

RIS consists of multiple reflecting elements that can reflect and adjust the incident electromagnetic waves [3]. RIS technology is experiencing rapid development. Recently, a rising beyond-diagonal (BD)-RIS architecture, which is also known as "RIS 2.0", has been proposed [8]-[9]. The BD-RIS extends the conventional RIS architecture by connecting different RIS elements with tunable impedance components and elevates the configuration flexibility. Specifically, from a viewpoint of scattering parameter network theory [3], the conventional diagonal RIS is indeed an impedance network with each of its port (i.e., RIS element) grounded through a reconfigurable impedance component. It is indeed an extremely simplified special case of BD-RIS architecture. The more generalized BD-RIS architecture possesses more powerful beamsteering capability. One typical BD-RIS implementation scheme is the fully-connected (FC) architecture [8]-[9], which connects each pair of RIS elements to achieve utmost beamforming gain. As demonstrated in [10], FC BD-RIS can boost the receiving signal power by 62% compared to the conventional diagonal RIS. The authors of [11], via utilizing manifold optimization techniques, investigate employing BD-RIS in wireless network to improve system's spectral efficiency and manifest the advantageous beamforming gain of BD-RIS over its diagonal counterpart.

Enlightened by the exciting advancement of BD-RIS technique, we are motivated to exploit BD-RIS to further enhance ISAC system performance. The contributions of this paper are specified as follows:

- This paper investigates leveraging BD-RIS technology to enhance the throughput performance in ISAC networks. One predominant challenge of this study lies in the coexistence of the orthogonality condition due to BD-RIS architecture and the nonconvex quartic sensing constraint, which makes our problem much more challenging than any existing relevant literature, e.g., [4]-[11]).
- To resolve the challenge, by appropriately introducing splitting variables and employing penalty-dual-decomposition (PDD) technique, we successfully decouple the orthogonality condition from others and degrade the quartic constraint into quadratic ones, which yields an algorithm updating each variable efficiently.
- Numerical results are provided to demonstrate the effectiveness of our proposed algorithm and the benefit of BD-RIS over the conventional diagonal RIS.

II. Problem Formulation

In this paper, we consider a multi-user MISO ISAC system aided by FC BD-RIS as shown in Fig. 1. The dual-functional BS is equipped with uniform linear array (ULA) with M antennas for transmitting and receiving and serves K single-antenna mobile users. Besides communication, the BS also intends to simultaneously sense a potential target located in a specific direction. The transmit signal at the BS can be given as:

$$\boldsymbol{x} = \boldsymbol{W}_c \boldsymbol{s}_c + \boldsymbol{W}_r \boldsymbol{s}_r, \tag{1}$$

The work of Yang Liu is supported by the Open Research Project Program of the State Key Laboratory of Internet of Things for Smart City (University of Macau) (Ref. No.: SKLIoTSC(UM)-2021-2023/ORP/GA01/2022). Q. Wu's work is supported by National Key RD Program of China (2022YFB2903500), NSFC 62371289 and NSFC 62331022. Corresponding author: Yang Liu.

Z. Liu and Y. Liu are with the School of Information and Communication Engineering, Dalian University of Technology, Dalian, China, email: liuzr1999@mail.dlut.edu.cn, yangliu_613@dlut.edu.cn

Shanpu Shen is with the Department of Electrical Engineering and Electronics, University of Liverpool, Liverpool L69 3GJ, U.K. (email: Shanpu.Shen@liverpool.ac.uk).

Q. Wu is with Department of Electronic Engineering, Shanghai Jiao Tong University, Shanghai, China, email: qingqingwu@sjtu.edu.cn.

Q. Shi is with the School of Software Engineering, Tongji University, Shanghai, China, and also with the Shenzhen Research Institute of Big Data, Shenzhen, China, email: shiqj@tongji.edu.cn.

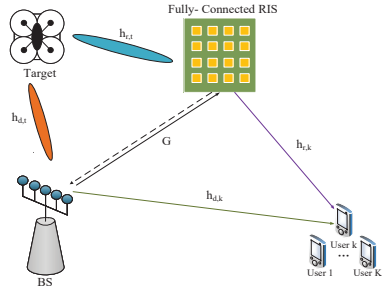

Fig. 1. A FC BD-RIS aided ISAC system.

where $\boldsymbol{W}_c \in \mathbb{C}^{M\times K}$ is the communication precoder with its k-th column $\boldsymbol{w}_k$ being the beamformer for the k-th user, $\boldsymbol{W}_r \in \mathbb{C}^{M\times M}$ denotes the sensing precoder and $\boldsymbol{s}_c \in \mathbb{C}^{K\times 1}$ and $\boldsymbol{s}_r \in \mathbb{C}^{M\times 1}$ represent the information and probing symbols, respectively. It is assumed that that information and probing symbols have zero mean, unit covariance and are mutually uncorrelated, i.e., $\mathbb{E}\left\{\boldsymbol{s}_c\boldsymbol{s}_c^H\right\} = \boldsymbol{I}_K$, $\mathbb{E}\left\{\boldsymbol{s}_r\boldsymbol{s}_r^H\right\} = \boldsymbol{I}_M$ and $\mathbb{E}\left\{\boldsymbol{s}_c\boldsymbol{s}_r^H\right\} = \boldsymbol{O}_{K\times M}$ where $\mathbb{E}\{\cdot\}$ denotes expectation. For simplicity, we define $\boldsymbol{W} \triangleq [\boldsymbol{W}_c, \boldsymbol{W}_r]$ and $\boldsymbol{s} \triangleq [\boldsymbol{s}_c^T, \boldsymbol{s}_r^T]^T$. The channel coefficients between the BS and the RIS, the BS to the k-th user, and the RIS to the k-th user are represented respectively by $\boldsymbol{G} \in \mathbb{C}^{N\times M}$, $\boldsymbol{h}_{d,k} \in \mathbb{C}^{M\times 1}$ and $\boldsymbol{h}_{r,k} \in \mathbb{C}^{N\times 1}$. To enhance performance, an N-element fully-connected BD-RIS ($\boldsymbol{\Phi} \in \mathbb{C}^{N\times N}$) is deployed in the network. Due to its fully-connected impedance networking architecture [11], the BD-RIS configuration matrix $\boldsymbol{\Phi}$ should satisfy $\boldsymbol{\Phi}^T = \boldsymbol{\Phi}$ and $\boldsymbol{\Phi}\boldsymbol{\Phi}^H = \boldsymbol{I}_N$. The received signal at the k-th user is :

$$y_k = (\boldsymbol{h}_{d,k}^H + \boldsymbol{h}_{r,k}^H\boldsymbol{\Phi}\boldsymbol{G})\boldsymbol{x} + n_k, \forall k, \tag{2}$$

where n_k is the receiving noise and $n_k \sim \mathcal{CN}(0, \sigma_k^2)$. We denote the effective channel $\boldsymbol{h}_k^H \in \mathbb{C}^{1\times M}$ between the BS and user k as $\boldsymbol{h}_k^H = \boldsymbol{h}_{d,k}^H + \boldsymbol{h}_{r,k}^H\boldsymbol{\Phi}\boldsymbol{G}$. Based on the above discussion, the k-th user's receiving SINR is

$$\mathsf{SINR}_k(\boldsymbol{W}, \boldsymbol{\Phi}) = \frac{|\boldsymbol{h}_k^H\boldsymbol{w}_k|^2}{\sum_{i=1,i\neq k}^{K+M}|\boldsymbol{h}_k^H\boldsymbol{w}_i|^2 + \sigma_k^2}. \tag{3}$$

At the same time, taking into account the reciprocity of the channel, the echo signal $\boldsymbol{y}_r \in \mathbb{C}^{M\times 1}$ reflected back from the sensing target is given by

$$\boldsymbol{y}_r = \alpha_t(\boldsymbol{h}_{d,t}^* + \boldsymbol{G}^T\boldsymbol{\Phi}^T\boldsymbol{h}_{r,t}^*)(\boldsymbol{h}_{d,t}^H + \boldsymbol{h}_{r,t}^H\boldsymbol{\Phi}\boldsymbol{G})\boldsymbol{x} + \boldsymbol{n}_r, \tag{4}$$

where $\boldsymbol{h}_{d,t} \in \mathbb{C}^{M\times 1}$ and $\boldsymbol{h}_{r,t} \in \mathbb{C}^{N\times 1}$ denote the BS-target and RIS-target channel, respectively, α_t represents the reflection cross section (RCS) coefficient with mean power $\mathbb{E}\left\{|\alpha_t|^2\right\} = \sigma_t^2$, and the receiving noise $\boldsymbol{n}_r \sim \mathcal{CN}(\boldsymbol{0}, \sigma_r^2\boldsymbol{I}_M)$. After receiving the echo, the BS removes the communication signal and utilizes a linear filter $\boldsymbol{u} \in \mathbb{C}^{M\times 1}$ to perform post-processing. Assuming perfectly cancelling out the communication signals from the echo, the signal-to-noise ration (SNR) of the filtered sensing signal is given by

$$\mathsf{SNR}_t(\boldsymbol{u}, \boldsymbol{W}, \boldsymbol{\Phi}) = \frac{\sigma_t^2\boldsymbol{u}^H\boldsymbol{H}_t(\boldsymbol{\Phi})\boldsymbol{W}_r\boldsymbol{W}_r^H\boldsymbol{H}_t^H(\boldsymbol{\Phi})\boldsymbol{u}}{\sigma_r^2\boldsymbol{u}^H\boldsymbol{u}}, \tag{5}$$

where $\boldsymbol{H}_t(\boldsymbol{\Phi}) \triangleq (\boldsymbol{h}_{d,t}^* + \boldsymbol{G}^T\boldsymbol{\Phi}^T\boldsymbol{h}_{r,t}^*)(\boldsymbol{h}_{d,t}^H + \boldsymbol{h}_{r,t}^H\boldsymbol{\Phi}\boldsymbol{G})$ denotes the equivalent channel for sensing.

In the above context, we intend to jointly design the linear filter $\boldsymbol{u}$, the beamforming $\boldsymbol{W}$ and the BD-RIS configuration $\boldsymbol{\Phi}$ to accomplish both communication and sensing functions. Specifically, our goal is to maximize the networks' throughput while guaranteeing a satisfactory radar sensing quality, which yields the following optimization problem:

$$\begin{aligned}(\mathrm{P0}): \quad \max_{\boldsymbol{u},\boldsymbol{W},\boldsymbol{\Phi}} \ & \sum_{k=1}^K \log(1+\mathsf{SINR}_k) \\ \text{s.t. } & \mathsf{SNR}_t(\boldsymbol{u},\boldsymbol{W},\boldsymbol{\Phi}) \geq \gamma, && \text{(6a)} \\ & \boldsymbol{\Phi}^H\boldsymbol{\Phi} = \boldsymbol{I}_N, \boldsymbol{\Phi} = \boldsymbol{\Phi}^T, && \text{(6b)} \\ & ||\boldsymbol{W}||_F^2 \leq P, && \text{(6c)}\end{aligned}$$

where γ is a predefined sensing SNR level, P is the BS transmit power budget and (6b) is due to the architecture of FC BD-RIS. Note constraint (6a) is quartic in $\boldsymbol{\Phi}$ and (6b) involves orthogonality condition, which makes our problem highly difficult.

III. Proposed Algorithm

In this section, we will tackle the problem (P0). Firstly, we leverage Lagrangian dual transform [13, Thm. 3] and quadratic transform [12, Cor. 1] to make the objective function more tractable, which yields the equivalent form in (7), shown at the bottom of this page, with r_k and c_k being the introduced intermediate variables. Next, we adopt block coordinate ascent (BCA) method to alternatively update different variables.

A. Update of $\{r_k\}$ and $\{c_k\}$

When other variables are fixed, the updates of the introduced intermediate variables $\{r_k\}$ and $\{c_k\}$ are indeed unconstrained concave maximization problems, whose closed-form solution can be readily obtained via taking derivative to zero, which yields:

$$r_k^\star = \frac{|\boldsymbol{h}_k^H\boldsymbol{w}_k|^2}{\sum_{i\neq k}^{K+M}|\boldsymbol{h}_k^H\boldsymbol{w}_i|^2 + \sigma_k^2}, c_k^\star = \frac{\sqrt{1+r_k}\boldsymbol{h}_k^H\boldsymbol{w}_k}{\sum_{i=1}^{K+M}|\boldsymbol{h}_k^H\boldsymbol{w}_i|^2 + \sigma_k^2}. \tag{8}$$

B. Update of $\boldsymbol{u}$

For the update of $\boldsymbol{u}$, since it only appears in the constraint (6a), the problem reduces to maximizing the sensing SNR with respect to (w.r.t.) $\boldsymbol{u}$. Therefore, the update of $\boldsymbol{u}$ reduces to solving the following problem:

$$(\mathrm{P1}): \quad \max_{\boldsymbol{u}} \ \frac{\sigma_t^2\boldsymbol{u}^H\boldsymbol{H}_t(\boldsymbol{\Phi})\boldsymbol{W}_r\boldsymbol{W}_r^H\boldsymbol{H}_t^H(\boldsymbol{\Phi})\boldsymbol{u}}{\sigma_r^2\boldsymbol{u}^H\boldsymbol{u}}.$$

The above problem is Rayleigh quotient maximization and by Rayleigh-Rits theorem, the optimal $\boldsymbol{u}$ should be aligned with the eigenvector associated with the largest eigenvalue of $\boldsymbol{H}_t(\boldsymbol{\Phi})\boldsymbol{W}_r\boldsymbol{W}_r^H\boldsymbol{H}_t^H(\boldsymbol{\Phi})$.

Note that although $\boldsymbol{u}$ does not directly impact on the objective value, its update promotes the sensing SNR and makes the problem more "feasible". This indeed provides larger margin for the update of other variables and in turn objective value improvement.

C. Update of $\boldsymbol{W}$

When other variables are given, we proceed to consider the optimization of $\boldsymbol{W}$. To simplify the subsequent discussions, according to the properties of the block-diagonal matrix, we introduce the following notations:

$$c_{w1} \triangleq \sum_{k=1}^K \left(\log(1+r_k) - r_k - |c_k|^2\sigma_k^2\right), \tag{9a}$$

$$\sum_{k=1}^K \log(1+r_k) - r_k - |c_k|^2\sigma_k^2 + 2\sqrt{1+r_k}\mathsf{Re}\left\{c_k^*\boldsymbol{h}_k^H\boldsymbol{w}_k\right\} - |c_k|^2\sum_{i=1}^{K+M}|\boldsymbol{h}_k^H\boldsymbol{w}_i|^2 \tag{7}$$

$$c_{w2} \triangleq \frac{\gamma_r \sigma_r^2 \boldsymbol{u}^H \boldsymbol{u}}{\sigma_t^2},\ \boldsymbol{A}_k \triangleq \underbrace{\mathsf{blkdiag}(\boldsymbol{h}_k \boldsymbol{h}_k^H, \ldots, \boldsymbol{h}_k \boldsymbol{h}_k^H)}_{K+M \text{ blocks}}, \quad (9b)$$

$$\boldsymbol{a}^H \triangleq \left(2\sqrt{1+r_1} c_1^* \boldsymbol{h}_1^H, \ldots, 2\sqrt{1+r_k} c_k^* \boldsymbol{h}_k^H, \boldsymbol{0}_M^T\right), \quad (9c)$$

$$\boldsymbol{w} \triangleq \mathsf{vec}(\boldsymbol{W}),\ \boldsymbol{B} \triangleq \sum\nolimits_{k=1}^{K} |c_k|^2 \boldsymbol{A}_k. \quad (9d)$$

where $\mathsf{vec}\{\cdot\}$ denotes the vectorization operation.

Based on the above notations, the subproblem to optimize $\boldsymbol{W}$ can be rewritten as follows:

$$\begin{aligned}(\mathrm{P2}): \quad \min_{\boldsymbol{w}} \quad & \boldsymbol{w}^H \boldsymbol{B} \boldsymbol{w} - \mathsf{Re}(\boldsymbol{a}^H \boldsymbol{w}) \\ \text{s.t.} \quad & -\|\boldsymbol{u}^H \boldsymbol{H}_t(\boldsymbol{\Phi}) \boldsymbol{W}_r\|_2^2 \le -c_{w2}, \quad (10a) \\ & \|\boldsymbol{w}\|_2^2 \le P. \quad (10b)\end{aligned}$$

The problem (P2) is nonconvex due to the constraint (10a). To overcome this difficulty, we leverage the majorization-minimization (MM) method [14]. Since the negative norm square term is concave, we can obtain its tight convex upper-bound via linearizing it at the point of $\boldsymbol{W} = \boldsymbol{W}_r^{(t)}$ with $\boldsymbol{W}_r^{(t)}$ being the value of $\boldsymbol{W}_r$ in the last iteration:

$$\begin{aligned}&-\|\boldsymbol{u}^H \boldsymbol{H}_t(\boldsymbol{\Phi}) \boldsymbol{W}_r\|_2^2 \le -\|\boldsymbol{u}^H \boldsymbol{H}_t(\boldsymbol{\Phi}) \boldsymbol{W}_r^{(t)}\|_2^2 \\ &-2\mathsf{Re}\left\{\mathsf{Tr}[(\boldsymbol{W}_r^{(t)})^H \boldsymbol{H}_t^H(\boldsymbol{\Phi}) \boldsymbol{u}\boldsymbol{u}^H \boldsymbol{H}_t(\boldsymbol{\Phi})(\boldsymbol{W}_r - \boldsymbol{W}_r^{(t)})]\right\}. \quad (11)\end{aligned}$$

By replacing the negative squared norm term in (10a) by the above upperbound, (P2) becomes convex and solvable.

D. Update of $\boldsymbol{\Phi}$

In this subsection, we investigate the update of $\boldsymbol{\Phi}$, which aims at solving the following problem:

$$\begin{aligned}(\mathrm{P3}): \quad \min_{\boldsymbol{\Phi}} \quad & g(\boldsymbol{\Phi}) \\ \text{s.t.} \quad & \mathsf{SNR}_t(\boldsymbol{\Phi}) \ge \gamma, \boldsymbol{\Phi} = \boldsymbol{\Phi}^T \quad (12a) \\ & \boldsymbol{\Phi}^H \boldsymbol{\Phi} = \boldsymbol{I}_N, \quad (12b)\end{aligned}$$

where the explicit expression of $g(\boldsymbol{\Phi})$ is detailed (13) which utilizes $\mathrm{Tr}(\boldsymbol{AB}) = \mathrm{Tr}(\boldsymbol{BA})$ and $\mathsf{SNR}_t(\boldsymbol{\Phi})$ is given in (5), where $\boldsymbol{W}$ and $\boldsymbol{u}$ are regarded as constants. To attack (P3), two prominent difficulties arise: i) $\mathsf{SNR}_t(\boldsymbol{\Phi})$ is a quartic function in $\boldsymbol{\Phi}$; ii) the orthogonality condition (12b) is highly nonconvex. To deal with the first challenge, we rewrite the round-trip effective channel $\boldsymbol{H}_t(\boldsymbol{\Phi})$ as follows:

$$\boldsymbol{H}_t(\boldsymbol{\Phi}, \boldsymbol{\Phi}_2) = (\boldsymbol{h}_{d,t}^* + \boldsymbol{G}^T \boldsymbol{\Phi}^T \boldsymbol{h}_{r,t}^*)(\boldsymbol{h}_{d,t}^H + \boldsymbol{h}_{r,t}^H \boldsymbol{\Phi}_2 \boldsymbol{G}), \quad (14)$$

where $\boldsymbol{\Phi} = \boldsymbol{\Phi}_2$. By introducing the copy $\boldsymbol{\Phi}_2$ of $\boldsymbol{\Phi}$, we decompose the original quartic terms in (12a) into quadratic terms of $\boldsymbol{\Phi}$ and $\boldsymbol{\Phi}_2$, respectively, whose updates are more tractable. Besides, to make the orthogonality condition (12b) tractable, we introduce another copy $\boldsymbol{\Phi}_1$ of $\boldsymbol{\Phi}$ to decouple (12b) from other constraints. In the following, we adopt PDD methodology [15] to tackle the above problem. Firstly, to decouple the update of $\boldsymbol{\Phi}$, $\boldsymbol{\Phi}_1$ and $\boldsymbol{\Phi}_2$, we turn to consider the augmented Lagrangian (AL) problem of (P3). The AL problem omits the equality constraints $\boldsymbol{\Phi} = \boldsymbol{\Phi}_1$ and $\boldsymbol{\Phi} = \boldsymbol{\Phi}_2$ and punishes them in the objective function, which is given as:

$$\begin{aligned}(\mathrm{P4}): \min_{\boldsymbol{\Phi}, \boldsymbol{\Phi}_1, \boldsymbol{\Phi}_2} \ & g(\boldsymbol{\Phi}) + \frac{1}{2\rho} \sum\nolimits_{i=1}^{2} \|\boldsymbol{\Phi} - \boldsymbol{\Phi}_i\|_F^2 \\ & + \sum\nolimits_{i=1}^{2} \mathsf{Re}\left\{\mathsf{Tr}[\boldsymbol{\Lambda}_i^H (\boldsymbol{\Phi} - \boldsymbol{\Phi}_i)]\right\} \\ \text{s.t.} \ & \boldsymbol{\Phi}_1^H \boldsymbol{\Phi}_1 = \boldsymbol{I}_N, \quad (15a) \\ & \mathsf{SNR}_t(\boldsymbol{\Phi}, \boldsymbol{\Phi}_2) \ge \gamma, \quad (15b) \\ & \boldsymbol{\Phi} = \boldsymbol{\Phi}^T, \boldsymbol{\Phi}_2 = \boldsymbol{\Phi}_2^T, \quad (15c)\end{aligned}$$

where $\{\boldsymbol{\Lambda}_i\}$ is the Lagrangian dual variable associated with the equation $\boldsymbol{\Phi} = \boldsymbol{\Phi}_i, i \in \{1, 2\}$, ρ is penalty parameter [15], and $\mathsf{SNR}_t(\boldsymbol{\Phi}, \boldsymbol{\Phi}_2)$ is obtained via substituting the $\boldsymbol{H}_t(\boldsymbol{\Phi})$ in $\mathsf{SNR}_t(\boldsymbol{\Phi})$ with $\boldsymbol{H}_t(\boldsymbol{\Phi}, \boldsymbol{\Phi}_2)$.

The PDD method is a two layer iterative procedure, with its inner alternatively updating $\boldsymbol{\Phi}$, $\boldsymbol{\Phi}_1$ and $\boldsymbol{\Phi}_2$ and its outer layer selectively adjusting ρ or $\{\boldsymbol{\Lambda}_i\}$. In the following, we will elaborate each block's update in full details.

1) Update of $\boldsymbol{\Phi}$: When $\boldsymbol{\Phi}_1$ and $\boldsymbol{\Phi}_2$ are fixed, we update $\boldsymbol{\Phi}$ by solving the following problem:

$$\begin{aligned}(\mathrm{P5}): \min_{\boldsymbol{\Phi}} \ & g(\boldsymbol{\Phi}) + \frac{1}{2\rho} \sum\nolimits_{i=1}^{2} \|\boldsymbol{\Phi} - \boldsymbol{\Phi}_i\|_F^2 \\ & + \sum\nolimits_{i=1}^{2} \mathsf{Re}\left\{\mathsf{Tr}[\boldsymbol{\Lambda}_i^H (\boldsymbol{\Phi} - \boldsymbol{\Phi}_i)]\right\} \\ \text{s.t.} \quad & \mathsf{SNR}_t(\boldsymbol{\Phi}|\boldsymbol{\Phi}_2) \ge \gamma, \ \boldsymbol{\Phi} = \boldsymbol{\Phi}^T. \quad (16)\end{aligned}$$

Since $\boldsymbol{\Phi}$ is symmetric, the independent variables are indeed its upper-triangular entries, which have dimension of $0.5N(N+1)$ and are denoted by a vector $\boldsymbol{\psi} \in \mathbb{C}^{0.5N(N+1)}$. Defining $\boldsymbol{\phi} \triangleq \mathsf{vec}(\boldsymbol{\Phi})$, $\boldsymbol{\phi}$ and $\boldsymbol{\psi}$ are connected via the identity

$$\boldsymbol{\phi} = \boldsymbol{K}_2 \boldsymbol{\psi}, \quad \boldsymbol{\psi} = \boldsymbol{K}_1 \boldsymbol{\phi}, \quad (17)$$

where $\boldsymbol{K}_1$ and $\boldsymbol{K}_2$ are reshaping matrices with their entries being 0 or 1 and can be easily determined.

Utilizing (17), $\|\boldsymbol{A}\|_F^2 = \mathrm{Tr}\left\{\boldsymbol{A}\boldsymbol{A}^H\right\}$ and $\mathrm{Tr}\{\boldsymbol{ABCD}\} = \mathrm{vec}^T(\boldsymbol{B})(\boldsymbol{C} \otimes \boldsymbol{A}^T)\mathrm{vec}(\boldsymbol{D})$, we rewrite (P5) w.r.t. $\boldsymbol{\psi}$ explicitly as follows:

$$\begin{aligned}(\mathrm{P6}): \quad \min_{\boldsymbol{\psi}} \ & \boldsymbol{\psi}^H \boldsymbol{Q} \boldsymbol{\psi} - 2\mathsf{Re}(\boldsymbol{q}^H \boldsymbol{\psi}) \\ \text{s.t.} \ & -\boldsymbol{\psi}^H \boldsymbol{Q}_2 \boldsymbol{\psi} - 2\mathsf{Re}(\boldsymbol{q}_2^H \boldsymbol{\psi}) \le -c_\phi, \quad (18)\end{aligned}$$

where the newly introduced coefficients are detailed in (19) at the topmost section of next page.

The problem (P6) is nonconvex due to (18). To make it tractable, we adopt MM method to linearize the nonconvex quadratic term as follows:

$$-\boldsymbol{\psi}^H \boldsymbol{Q}_2 \boldsymbol{\psi} \le -2\mathsf{Re}[(\boldsymbol{\psi}^{(t)})^H \boldsymbol{Q}_2 (\boldsymbol{\psi} - \boldsymbol{\psi}^{(t)})] - (\boldsymbol{\psi}^{(t)})^H \boldsymbol{Q}_2 \boldsymbol{\psi}^{(t)} \quad (20)$$

where $\boldsymbol{\psi}^{(t)}$ is the value of $\boldsymbol{\psi}$ in the last iteration. By convexifying (20) using the above upper bound, (P6) becomes convex and hence $\boldsymbol{\phi}$ (namely $\boldsymbol{\Phi}$) can be updated.

2) Update of $\boldsymbol{\Phi}_1$: When $\boldsymbol{\Phi}$ and $\boldsymbol{\Phi}_2$ are fixed, $\boldsymbol{\Phi}_1$ should be updated by solving the following problem:

$$\begin{aligned}(\mathrm{P7}): \min_{\boldsymbol{\Phi}_1} \ & \|\boldsymbol{\Phi}_1 - (\boldsymbol{\Phi} + \rho \boldsymbol{\Lambda}_1)\|_F^2 \\ \text{s.t.} \ & \boldsymbol{\Phi}_1^H \boldsymbol{\Phi}_1 = \mathbf{I}_N. \quad (21)\end{aligned}$$

Fortunately, (P7) has a closed form solution. Specifically, suppose that $\boldsymbol{\Phi} + \rho \boldsymbol{\Lambda}_1$ has singular value decomposition (SVD) $\boldsymbol{\Phi} + \rho \boldsymbol{\Lambda}_1 = \boldsymbol{U} \boldsymbol{\Sigma} \boldsymbol{V}^H$ with $\boldsymbol{U}$ and $\boldsymbol{V}$ being the left and right singular vectors. Then, according to Prop.7 [16], the optimal solution to (P7) is given as

$$\boldsymbol{\Phi}_1^\star = \boldsymbol{U} \boldsymbol{I}_N \boldsymbol{V}^H. \quad (22)$$

3) Update of $\boldsymbol{\Phi}_2$: The update of $\boldsymbol{\Phi}_2$ aims to solve the

$$g(\boldsymbol{\Phi}) \triangleq \mathrm{Tr}(\boldsymbol{E}\boldsymbol{\Phi}^H \boldsymbol{F} \boldsymbol{\Phi}) - \mathsf{Re}\left[\mathrm{Tr}(\boldsymbol{D}\boldsymbol{\Phi})\right], \quad \boldsymbol{E} \triangleq \sum\nolimits_{i=1}^{K+M} \boldsymbol{G}\boldsymbol{w}_i \boldsymbol{w}_i^H \boldsymbol{G}^H, \quad \boldsymbol{F} \triangleq \sum\nolimits_{i=1}^{K} |c_k|^2 \boldsymbol{h}_{r,k} \boldsymbol{h}_{r,k}^H, \quad (13a)$$

$$\boldsymbol{D} \triangleq \sum\nolimits_{k=1}^{K} 2\sqrt{1+r_k} c_k^* \boldsymbol{G}\boldsymbol{w}_k \boldsymbol{h}_{r,k}^H - \sum\nolimits_{k=1}^{K} |c_k|^2 \sum\nolimits_{i=1}^{K+M} 2\boldsymbol{G}\boldsymbol{w}_i \boldsymbol{w}_i^H \boldsymbol{h}_{d,k} \boldsymbol{h}_{r,k}^H. \quad (13b)$$

$$\boldsymbol{Q} = \boldsymbol{K}_2^H(\boldsymbol{F}\otimes\boldsymbol{E}^T)\boldsymbol{K}_2 + \rho^{-1}\boldsymbol{K}_2^H\boldsymbol{K}_2, \quad \boldsymbol{q}^H = 0.5\rho^{-1}\boldsymbol{\phi}_1^H\boldsymbol{K}_2 + 0.5\rho^{-1}\boldsymbol{\phi}_2^H\boldsymbol{K}_2 - 0.5vec^T(\boldsymbol{\Lambda}_1^H + \boldsymbol{\Lambda}_2^H - \boldsymbol{D})\boldsymbol{K}_2, \tag{19a}$$

$$\boldsymbol{Q}_2 = \boldsymbol{K}_2^H\left\{\boldsymbol{G}^*\boldsymbol{u}\boldsymbol{u}^H\boldsymbol{G}^T \otimes [\boldsymbol{h}_{r,t}(\boldsymbol{h}_{d,t}^T + \boldsymbol{h}_{r,t}^T\boldsymbol{\Phi}_2^*\boldsymbol{G}^*)\boldsymbol{W}_r^*\boldsymbol{W}_r^T(\boldsymbol{h}_{d,t}^* + \boldsymbol{G}^T\boldsymbol{\Phi}_2^T\boldsymbol{h}_{r,t}^*)\boldsymbol{h}_{r,t}^H]\right\}\boldsymbol{K}_2, \tag{19b}$$

$$\boldsymbol{q}_2^H = \mathsf{vec}^T[\boldsymbol{h}_{r,t}^*(\boldsymbol{h}_{d,t}^H + \boldsymbol{h}_{r,t}^H\boldsymbol{\Phi}_2\boldsymbol{G})\boldsymbol{W}_r\boldsymbol{W}_r^H(\boldsymbol{h}_{d,t} + \boldsymbol{G}^H\boldsymbol{\Phi}_2^H\boldsymbol{h}_{r,t})\boldsymbol{h}_{d,t}^T\boldsymbol{u}\boldsymbol{u}^H\boldsymbol{G}^T]\boldsymbol{K}_2, \tag{19c}$$

$$c_\phi = \sigma_t^{-2}\gamma_r\sigma_r^2\boldsymbol{u}^H\boldsymbol{u} - \boldsymbol{u}^H\boldsymbol{h}_{d,t}^*(\boldsymbol{h}_{d,t}^H + \boldsymbol{h}_{r,t}^H\boldsymbol{\Phi}_2\boldsymbol{G})\boldsymbol{W}_r\boldsymbol{W}_r^H(\boldsymbol{G}^H\boldsymbol{\Phi}_2^H\boldsymbol{h}_{r,t} + \boldsymbol{h}_{d,t})\boldsymbol{h}_{d,t}^T\boldsymbol{u}. \tag{19d}$$

$$\boldsymbol{Q}_3 = 0.5\rho^{-1}\boldsymbol{K}_2^H\boldsymbol{K}_2, \quad \boldsymbol{q}_3^H = \mathsf{vec}^T(0.5\rho^{-1}\boldsymbol{\Phi}^H + 0.5\boldsymbol{\Lambda}_2^H)\boldsymbol{K}_2, \tag{25a}$$

$$\boldsymbol{Q}_4 = \boldsymbol{K}_2^H\left\{[\boldsymbol{h}_{r,t}(\boldsymbol{h}_{d,t}^T + \boldsymbol{h}_{r,t}^T\boldsymbol{\Phi}^*\boldsymbol{G}^*)\boldsymbol{u}\boldsymbol{u}^H(\boldsymbol{h}_{d,t}^* + \boldsymbol{G}^T\boldsymbol{\Phi}^T\boldsymbol{h}_{r,t}^*)\boldsymbol{h}_{r,t}^H] \otimes \boldsymbol{G}^*\boldsymbol{W}_r^*\boldsymbol{W}_r^T\boldsymbol{G}^T\right\}\boldsymbol{K}_2, \tag{25b}$$

$$\boldsymbol{q}_4^H = \mathsf{vec}^T[\boldsymbol{G}\boldsymbol{W}_r\boldsymbol{W}_r^H\boldsymbol{h}_{d,t}(\boldsymbol{h}_{d,t}^T + \boldsymbol{h}_{r,t}^T\boldsymbol{\Phi}^*\boldsymbol{G}^*)\boldsymbol{u}\boldsymbol{u}^H(\boldsymbol{h}_{d,t}^* + \boldsymbol{G}^T\boldsymbol{\Phi}^T\boldsymbol{h}_{r,t}^*)\boldsymbol{h}_{r,t}^H]\boldsymbol{K}_2, \tag{25c}$$

$$c_{\phi 2} = \sigma_t^{-2}\gamma_r\sigma_r^2\boldsymbol{u}^H\boldsymbol{u} - \boldsymbol{u}^H(\boldsymbol{h}_{d,t}^* + \boldsymbol{G}^T\boldsymbol{\Phi}^T\boldsymbol{h}_{r,t}^*)\boldsymbol{h}_{d,t}^H\boldsymbol{W}_r\boldsymbol{W}_r^H\boldsymbol{h}_{d,t}(\boldsymbol{h}_{d,t}^T + \boldsymbol{h}_{r,t}^T\boldsymbol{\Phi}^*\boldsymbol{G}^*)\boldsymbol{u}. \tag{25d}$$

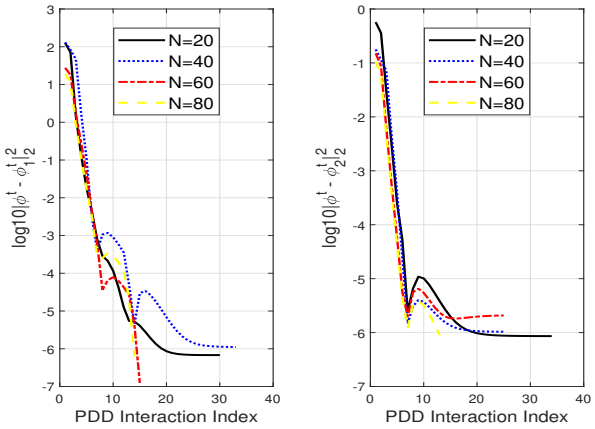

(a) Conv. of $\boldsymbol{\Phi}_1$ (b) Conv. of $\boldsymbol{\Phi}_2$

Fig. 2. Convergence of PDD method to update $\boldsymbol{\Phi}$.

following problem:

$$\text{(P8)}: \min_{\boldsymbol{\Phi}_2} \frac{1}{2\rho}\|\boldsymbol{\Phi} - \boldsymbol{\Phi}_2\|_F^2 + \mathsf{Re}\left\{\mathsf{Tr}\left[\boldsymbol{\Lambda}_2^H(\boldsymbol{\Phi} - \boldsymbol{\Phi}_2)\right]\right\}$$
$$\text{s.t.} \quad \mathsf{SNR}_t(\boldsymbol{\Phi}_2|\boldsymbol{\Phi}) \geq \gamma, \quad \boldsymbol{\Phi}_2 = \boldsymbol{\Phi}_2^T \tag{23}$$

Note $\boldsymbol{\Phi}_2$ is symmetric. Following similar lines to update $\boldsymbol{\Phi}$, we denote the upper-triangular elements of $\boldsymbol{\Phi}_2$ as $\boldsymbol{\psi}_2$ and $\boldsymbol{\phi}_2 \triangleq \mathsf{vec}(\boldsymbol{\Phi}_2)$. Utilizing the relation $\boldsymbol{\phi}_2 = \boldsymbol{K}_2\boldsymbol{\psi}_2$, we rewrite (P8) into an explicit form w.r.t. $\boldsymbol{\psi}_2$ as follows:

$$\text{(P9)}: \quad \min_{\boldsymbol{\psi_2}} \ \boldsymbol{\psi}_2^H\boldsymbol{Q}_3\boldsymbol{\psi}_2 - 2\mathsf{Re}(\boldsymbol{q}_3^H\boldsymbol{\psi}_2)$$
$$\text{s.t.} \ -\boldsymbol{\psi}_2^H\boldsymbol{Q}_4\boldsymbol{\psi}_2 - 2\mathsf{Re}(\boldsymbol{q}_4^H\boldsymbol{\psi}_2) \leq -c_{\phi 2}, \tag{24}$$

where the newly introduced coefficients are detailed in (25) at the topmost section of this page. Similar to (P6), (P9) can be effectively solved by first convexifying (24) via linearization. Details are omitted to avoid repitition. The inner layer of the PDD procedure alternatively updates $\boldsymbol{\Phi}$, $\boldsymbol{\Phi}_1$, and $\boldsymbol{\Phi}_2$ until converge is achieved. The outer layer will selectively update the Lagrangian multipliers $\{\boldsymbol{\Lambda}_i\}$ or the penalty parameter ρ. Specifically, if the equalities $\boldsymbol{\Phi} = \boldsymbol{\Phi}_i, i \in \{1,2\}$, are approximately satisfied within a satisfactory precision, we update the Lagrangian multipliers $\{\boldsymbol{\Lambda}_i\}$ as follows [15]:

$$\boldsymbol{\Lambda}_i = \boldsymbol{\Lambda}_i + \rho^{-1}(\boldsymbol{\Phi} - \boldsymbol{\Phi}_i), i \in \{1,2\}. \tag{26}$$

Otherwise, we inflate the penalty coefficient ρ^{-1}. The overall PDD procedure is summarized in Algorithm 1 and the whole procedure to solve (P0) is summarized in Algorithm 2.

Algorithm 1 PDD-Based Method to solve (P4)

Input: $\{\boldsymbol{h}_k\}_{k=1}^K$, γ, σ_t^2, σ_r^2, $\{\sigma_k\}_{k=1}^K$, $\boldsymbol{W}$, $\boldsymbol{u}$, $\{c_k\}_{k=1}^K$, $\{r_k\}_{k=1}^K$ and P.
Output: $\boldsymbol{\Phi}$.

```
initialize Φ^(0), Φ_1^(0), Φ_2^(0), Λ_1^(0), Λ_2^(0), ρ^(0) and k = 1 ;
vectorize Φ^(0), Φ_1^(0) and Φ_2^(0) to get φ^(0), φ_1^(0) and φ_2^(0) respectively;
extract ψ^(0) and ψ_2^(0) from φ^(0) and φ_2^(0) respectively;
repeat
    set ψ^(k-1,0) := ψ^(k-1), Φ_1^(k-1,0) := Φ_1^(k-1), ψ_2^(k-1,0) := ψ_2^(k-1), t = 0;
    repeat
        update ψ^(k-1,t+1) by solving (P6);
        update Φ_1^(k-1,t+1) by (22);
        update ψ_2^(k-1,t+1) by solving (P10); t++;
    until convergence
    set ψ^(k) := ψ^(k-1,∞), Φ_1^(k) := Φ_1^(k-1,∞), ψ_2^(k) := ψ_2^(k-1,∞)
    recover φ^(k) and φ_2^(k) from ψ^(k) and ψ_2^(k) respectively and
    vectorize Φ_1^(k) to get φ_1^(k);
    if ||φ^(k) - φ_i^(k)||_2 ≤ η_k, i = 1, 2 then
        Λ_i^(k+1) = Λ_i^(k) + (1/ρ^(k))(Φ^(k) - Φ_i^(k)), ρ^(k+1) = ρ^(k);
    else
        Λ_i^(k+1) = Λ_i^(k), ρ^(k+1) = c · ρ^(k);
    end if
    k++
until ||φ^(k) - φ_i^(k)||_2 is sufficiently small
recover the optimal Φ* from the optimal φ*
```

Algorithm 2 Solving the problem (P0)

Input: $\{\boldsymbol{h}_k\}_{k=1}^K$, γ, σ_t^2, σ_r^2, $\{\sigma_k\}_{k=1}^K$, $\{c_k\}_{k=1}^K$, $\{r_k\}_{k=1}^K$ and P.
Output: $\sum_{k=1}^K \log(1 + \mathsf{SINR}_k)$.

```
initialize u^(0), W^(0), Φ^(0), and t = 0;
repeat
    update r_k^(t+1) and c_k^(t+1) by function (8);
    update u^(t+1) by solving (P1);
    update W^(t+1) by solving (P2);
    update Φ^(t+1) by Alg.1;
    t := t + 1;
until convergence
```

IV. Simulation Results

In this section, we present numerical results validating our proposed solution. The experiment configures the BS with $M = 8$ antennas serving $K = 4$ mobile users. Heights are set at 2m for the BS, 4m for the fully-connected RIS,

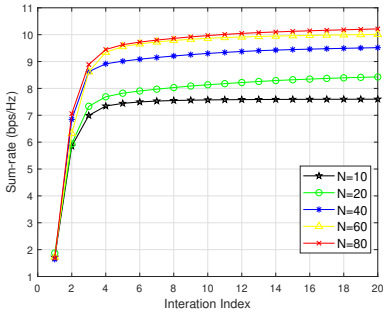

Fig. 3. Convergence of Alg. 2.

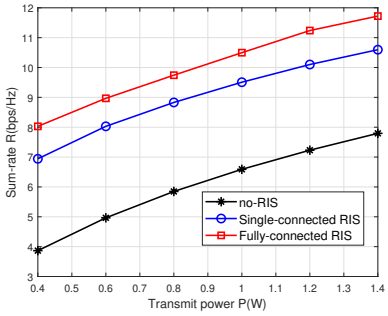

Fig. 4. Impact of transmit power P.

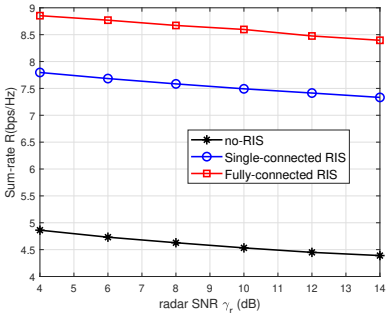

Fig. 5. Impact of sensing threshold γ_r.

and 1.5m for users. The RIS is positioned right above the BS and around 50m away from the users. The BS-IRS link follows Rician fading (Rician factor: 5 dB, fading exponent: 2.5), while BS-user and RIS-user links follow Rayleigh fading (fading exponents: 3.5 and 2.8, respectively). Line-of-sight paths exist for BS-target and RIS-target links. The target is at $\theta = 30°$, 25m away, with a pathloss fading exponent of 2.2. RCS is set at $\sigma_t^2 = 1$, and the sensing threshold is 10dB. Noise levels are $\sigma_r^2 = \sigma_k^2 = -80$dBm.

Firstly, Fig. 2 illustrates the convergence behavior of the PDD procedure to update $\mathbf{\Phi}$. Specifically, Fig. 2 illustrates the variation of the difference $\|\boldsymbol{\phi} - \boldsymbol{\phi}_1\|_2$ and $\|\boldsymbol{\phi} - \boldsymbol{\phi}_2\|_2$ (in log domain), respectively, along with the PDD iteration progress under different settings of the number of RIS elements (i.e., N). As shown in Fig. 2, the PDD algorithm generally converges very well within 20 interations with the thresholds being 10^{-6}. The convergence is insensible to N.

Fig. 3 depicts the convergence of Alg. 2 with different Ns. Algorithm 2 generally converges within 10 iterations and achieves over 90% of the optimization gain upon the very first three iterations. Besides, the beamforming gain increment exhibits marginal effect when N grows.

In Fig. 4, we illustrate the impact of transmit power budget of the BS. As shown in Fig. 4, the FC BD-RIS significantly outperforms the no-RIS scenario and yields approximately 15% sum-rate gain over the diagonal counterpart. This advantage is due to the non-diagonal structure of the BD-RIS reconfiguration matrix, which subsumes that of diagonal RIS as special case and hence yields much more powerful beamsteering capability.

Fig. 5 demonstrates fundamental trade-off between sensing and communication in spatial multiplexing. As shown in Fig. 5, when the sensing SNR threshold γ_r increases, communication rate drops. In fact, to fulfill higher sensing quality, beam vector should be more aligned with the target direction, which results in decreasing the receiving power of communication users. Thanks to the superior beamforming capability of BD-RIS, it exhibits advantageous sensing and communication trade-off over the conventional diagonal RIS.

V. Conclusions

This paper considers joint beamforming design in a fully-connected RIS assisted ISAC system. To tackle the optimization, which is highly difficult due to the quartic and orthogonality constraints, we introduce splitting variables and utilize PDD method to develop an effective solution. Extensive simulations verify the effectiveness of our proposed algorithm and the benefit of fully-connected RIS. For future work, other meaningful performance metrics, e.g., power consumption, energy efficiency and sensing SNR, could be considered in BD-RIS aided network.

References

[1] F. Liu, Y. Cui, et al. "Integrated sensing and communications: Toward dual-functional wireless networks for 6G and beyond," *IEEE J. Sel. Areas Commun.*, vol. 40, no. 6, pp. 1728-1767, Jun. 2022.

[2] J. A. Zhang, F. Liu, et al. "An overview of signal processing techniques for joint communication and radar sensing," *IEEE J. Sel. Topics Signal Process.*, vol. 15, no. 6, pp. 1295-1315, Nov. 2021.

[3] Q. Wu, S. Zhang, B. Zheng, C. You, and R. Zhang, "Intelligent reflecting surface-aided wireless communications: A tutorial," *IEEE Trans. Commun.*, vol. 69, no. 5, pp. 3313-3351, May 2021

[4] A. Aubry, A. De Maio, and M. Rosamilia, "Reconfigurable intelligent surfaces for N-LOS radar surveillance," *IEEE Trans. Veh. Technol.*, vol. 70, no. 10, pp. 10735–10749, Oct. 2021.

[5] X. Wang, Z. Fei, J. Guo, Z. Zheng, and B. Li, "RIS-assisted spectrum sharing between MIMO radar and MU-MISO communication systems," *IEEE Wireless Commun. Lett.*, vol. 10, no. 3, pp. 594–598, Mar. 2021.

[6] Y. Guo, Yang Liu, et al. "Joint Beamforming and Power Allocation for RIS Aided Full-Duplex Integrated Sensing and Uplink Communication System," *IEEE Trans. Wireless Commun.*, early access, 2023

[7] X. Song, J. Xu, F. Liu, T. X. Han and Y. C. Eldar, "Intelligent Reflecting Surface Enabled Sensing: Cramér-Rao Bound Optimization," *IEEE Trans. Signal Process.*, vol. 71, pp. 2011-2026, 2023

[8] S. Shen, et al. "Modeling and architecture design of reconfigurable intelligent surfaces using scattering parameter network analysis," *IEEE Trans. Wireless Commun.*, vol. 21, no. 2, pp. 1229-1243, Feb. 2022.

[9] H. Li, S. Shen, M. Nerini and B. Clerckx, "Reconfigurable intelligent surfaces 2.0: Beyond diagonal phase shift matrices," *early access*, 2023, doi: 10.1109/MCOM.001.2300019.

[10] M. Nerini, S. Shen and B. Clerckx, "Closed-form global optimization of beyond diagonal reconfigurable intelligent surfaces," *IEEE Trans. Wireless Commun.*, 2023. Early Access.

[11] H. Li, et al. "Beyond diagonal reconfigurable intelligent surfaces: From transmitting and reflecting modes to single-, group-, and fully-connected architectures," *IEEE Trans. Wireless Commun.*, vol. 22, no. 4, pp. 2311-2324, Apr. 2023. Available: https://arxiv.org/abs/2209.00301

[12] K. Shen and W. Yu, "Fractional programming for communication systems-part I: Power control and beamforming," *IEEE Trans. Signal Process.*, vol. 66, no. 10, pp. 2616-2630, May. 2018

[13] —, Part II: Uplink scheduling via matching," *IEEE Trans. Signal Process.*, vol. 66, no. 10, pp. 2631–2644, Mar. 2018

[14] Y. Sun, P. Babu, and D. P. Palomar, "Majorization-minimization algorithms in signal processing, communications, and machine learning," *IEEE Trans. Signal Process.*, vol. 65, no. 3, pp. 794¨C816, Feb. 2017.

[15] Q. Shi, and M. Hong, "Penalty dual decomposition method for smooth nonconvex optimization-part i: Algorithms and convergence analysis," *IEEE Trans. Signal Process.*, vol. 68, pp. 4108-4122, Jun. 2020.

[16] J. H. Manton, "Optimization algorithms exploiting unitary constraints," *IEEE Trans. Signal Process.*, vol. 50, no. 3, pp. 635-650, Mar. 2002.